Metabolic reprogramming in RCC tumors contributes to a dysfunctional immune response and immune exhaustion within the tumor microenvironment.

AUTHORS: **Lakshmi Chandramohan**, Sergio Hernandez, Brigitte Lovell, Lisa Duncan, Courtney Todorov, Harry Nunns, Jiong Fei, Judy Kuo, Erinn Parnell, and Qingyan Au.

NeoGenomics Laboratories, Houston, TX & Aliso Viejo, CA

Abstract #6745

Introduction

Renal cell carcinoma (RCC) represents 2–3% of global cancer diagnoses and 85% of all kidney neoplasms with the most common histological subtype being clear cell renal cell carcinoma (ccRCC)[1], an immunologically and histologically diverse tumor associated with poor clinical outcomes. While significant progress has been made in the development of immunotherapy for ccRCC, there are still many unanswered questions regarding mechanisms of immune evasion and resistance, and the development of predictive biomarkers for optimal treatment strategies for individual patients. Emerging evidence suggests that metabolic reprogramming marked by dynamic shifts in nutrient utilization extending beyond canonical Warburg physiology to include lipid anabolism, nutrient scavenging, catabolic pathways and microenvironment-driven metabolic plasticity, is central to overall ccRCC pathogenesis. We investigated the phenotype, functional states, and metabolic competencies of RCC immune cell populations, evaluating their potential associations with tumor clinicopathological features and stage-specific metabolic conditions.

Methodology

A retrospective analysis was performed on biopsied FFPE samples from 16 ccRCC patients across all clinical TNM stages (Stages I-IV). The spatial Paletrra™ workflow (NeoGenomics Laboratories, Inc.) with enhanced whole tissue capability coupled to the nCounter® Metabolic Pathways Panel were used to thoroughly investigate the complex interplay between the immunogenic nature of ccRCC tumors and metabolic reprogramming (Figure 1).

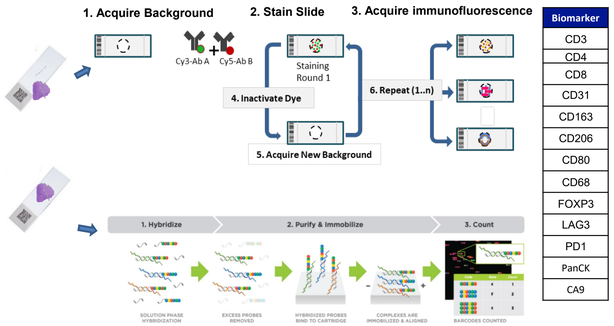

Biomarker
CD3
CD4
CD8
CD31
CD163
CD206
CD80
CD68
FOXP3
LAG3
PD1
PanCK
CA9

Figure 1: *Integrating metabolic gene expression analysis and end-to-end spatial Paletrra™. Sequential FFPE slides representing stages I-IV of ccRCC tumors were either tested using nCounter® analysis system or stained using the Paletrra™ workflow. For NanoString testing, RNA was extracted from FFPE slides and tested using* nCounter® *Metabolic Pathways panel. Normalized data was analyzed using proprietary bioinformatic tools. For each round of staining, conjugated fluorescent antibodies were applied to the slide, followed by imaging acquisition of stained slides. The dye was erased, enabling a second round of staining with another pair of fluorescent antibodies. Samples were imaged using the RareCyte CyteFinder® II HT whole slide imaging platform.*

Transcriptomic and proteomic analysis of ccRCC I-IV

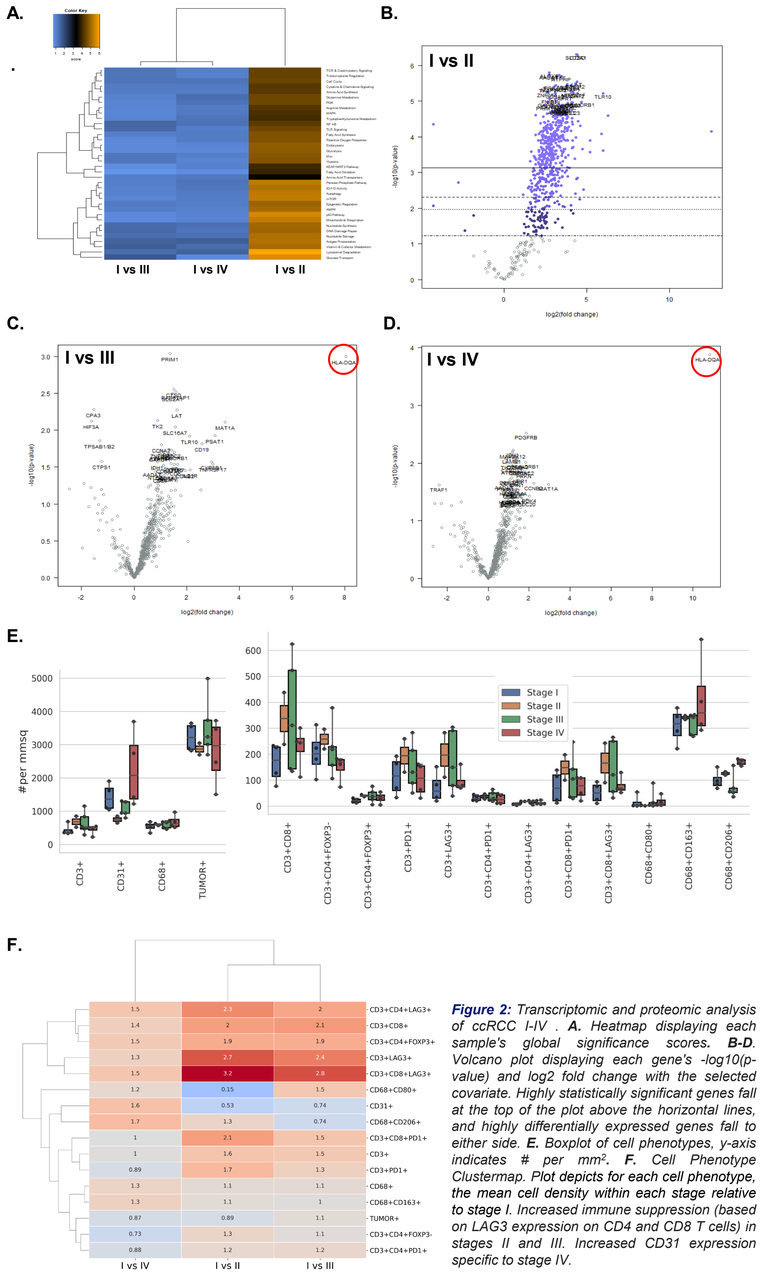

Figure 2: *Transcriptomic and proteomic analysis of ccRCC I-IV . **A.** Heatmap displaying each sample's global significance scores. **B-D.** Volcano plot displaying each gene's -log10(p-value) and log2 fold change with the selected covariate. Highly statistically significant genes fall at the top of the plot above the horizontal lines, and highly differentially expressed genes fall to either side. **E.** Boxplot of cell phenotypes, y-axis indicates # per mm². **F.** Cell Phenotype Clustermap. Plot depicts for each cell phenotype, the mean cell density within each stage relative to stage I. Increased immune suppression (based on LAG3 expression on CD4 and CD8 T cells) in stages II and III. Increased CD31 expression specific to stage IV.*

Spatial analysis across ccRCC stages I-IV

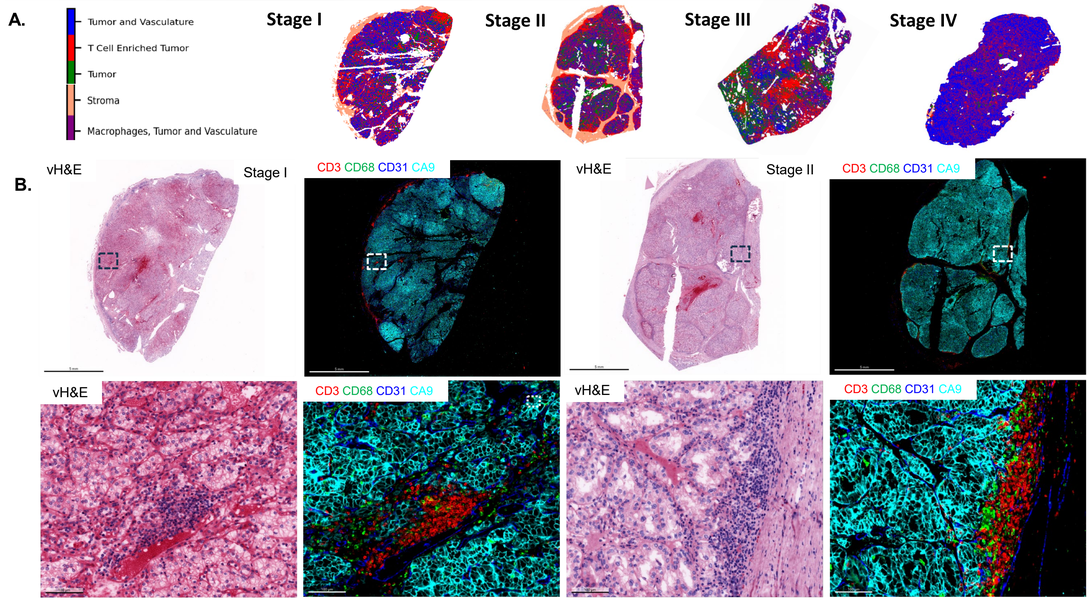

Figure 3. *Spatial analysis across ccRCC stages I-IV. **A.** Neighborhood overlay representative images showing tumor and vasculature (blue), T cell enriched tumor (red), tumor (green), stroma (pink), or macrophages, tumor, and vasculature (purple) regions in stage I-IV ccRCC samples. **B.** Whole slide imaging allows for visualization and characterization of the TME in ccRCC samples. Magnified views correspond to the dotted boxes to reveal detailed resolution of immune (CD3+ T cell, CD68+ macrophage), endothelial (CD31+), and tumor (CA9+) expression in Stage I and Stage II samples. **C.** Representative color overlay images showing comparison of macrophage (CD68+ CD163+), endothelial (CD31+), or LAG3+ T helper (CD4+) or T cytotoxic (CD8) cell expression between different ccRCC stages.*

Conclusions

- Observed increase in antigen presentation targets especially HLA-DRB1, with decreased chemokine and cytokine expression in ccRCC stage IV tumors.
- Increased immune suppression (based on LAG3 expression on CD4 and CD8 T cells) in stages II and III.
- Immune exhaustion phenotypes increasing in stage II through stage III. Increased vascularization in stage IV.

1. Salgia et al., 2024. https://ascopubs.org/doi/10.1200/EDBK_438642. Renal Cell Carcinoma of Variant Histology: New Biologic Understanding Leads to Therapeutic Advances

Lakshmi.chandramohan@neogenomics.com